Modulational instability in a fiber soliton ring laser induced by periodic dispersion variation

D. Y. Tang
Centre for Laser Science, Physics Department, The University of Queensland, Brisbane, Queensland 4072, Australia

W. S. Man, H. Y. Tam, and M. S. Demokan
Electrical Engineering Department, The Hong Kong Polytechnic University, Hung Hom, Kowloon, Hong Kong
(Received 2 March 1999; published 6 January 2000)

Modulational instability with sideband generation is experimentally observed in a passively mode-locked fiber soliton ring laser. We show numerically that this modulational instability is induced by the periodic dispersion variation experienced by light circulating in the laser cavity. Modulational instability caused by cross-phase-modulation is also observed in the laser and confirmed numerically.

PACS number(s): 42.55.Wd, 42.65.Sf, 42.65.Tg, 42.81.Dp

I. INTRODUCTION

Modulational instability is the well-known tendency in anomalous dispersion fibers for small variations in an almost constant power level to grow exponentially. Modulational instability of light waves in a single-mode optical fiber was first observed by Tai *et al.* [1]. Agrawal [2] has studied modulational instability in an erbium-doped fiber amplifier. He found that the existence of internal gain could lower the threshold for the modulational instability considerably compared with the case of undoped fibers. Recently, Smith and Doran [3] have theoretically analyzed the occurrence of modulational instability in fibers with periodic dispersion management. They found that the periodic dispersion variation in the fiber modifies the gain spectrum of the classic modulational instability. In the case of small periodic dispersion variations, a set of resonance occurs in the gain spectrum. Modulational instability induced by the periodic dispersion variation has been experimentally observed in a long-distance fiber transmission system [4]. Matera *et al.* [5] have studied the modulational instability of fibers under conditions of periodic power variation. They have observed a similar sideband generation as in the case of periodic dispersion variation, however the strength of this generated sideband is small. In this paper we report on an experimental observation of modulational instability with sideband generation in a passively mode-locked fiber soliton ring laser. We first show experimentally that for a fiber soliton laser because of the soliton energy quantization effect [6], increasing pump power of the laser will not increase the soliton energy but the strength of the dispersive waves. As the dispersive waves are linear waves, they are intrinsically unstable against modulational instability. When their strength becomes strong enough, they become unstable and consequently produce new discrete spectral components in the soliton spectrum. The new spectral components have large wavelength shifts in relation to the unstable dispersive wave spectra, which cannot be explained by the classic modulational instability. We then further show numerically that this observed modulational instability is a result of the periodic dispersion variation experienced by light circulating in the laser cavity. Modulational instability caused by cross-phase-modulation has also been experimentally observed in the laser and confirmed numerically.

II. EXPERIMENTAL SETUP AND RESULTS

The fiber soliton ring laser used in our experiment is schematically shown in Fig. 1, which has a similar configuration to that reported in [7,8]. The cavity length of the laser is about 12 m long, which is comprised of a 4-m-long erbium-doped fiber (Er^{+} concentration $\sim$ 2000 ppm) with a group velocity dispersion of about -10 ps/nm km and two pieces of 4-m-long single-mode dispersion-shifted fiber, whose group velocity dispersion is -2 ps/nm km. A polarization-dependent isolator is included in the cavity to enforce unidirectional operation. The nonlinear polarization rotation technique [9] is used to achieve self-started mode locking of the laser. To this end two polarization controllers, one consisting of two quarter-wave plates and the other of two quarter-wave plates and one half-wave plate, are used to control the polarization state of the light before and after the isolator. The two polarization controllers and the polarization-dependent isolator are mounted on a fiber bench, which makes the accurate adjustment of the polarization state of the light easier. A pigtailed InGaAsP laser diode operating at 1480 nm is used to pump the laser. The pump power is coupled into the laser cavity through a wavelength-division-multiplexing (WDM) coupler, and the pump power is continuously adjustable. The output of the laser is taken via a 10% fiber coupler and ana-

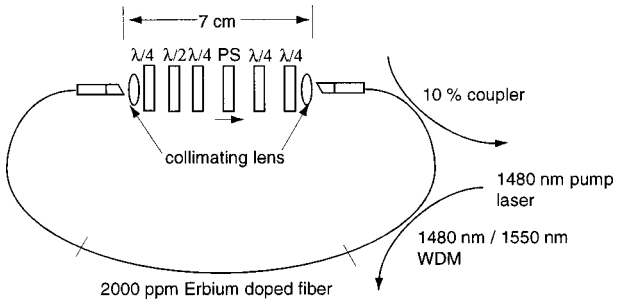

FIG. 1. Schematic of the experimental configuration. λ/4, quarter-wave plate; λ/2, half-wave plate; PS, polarization-dependent isolator.

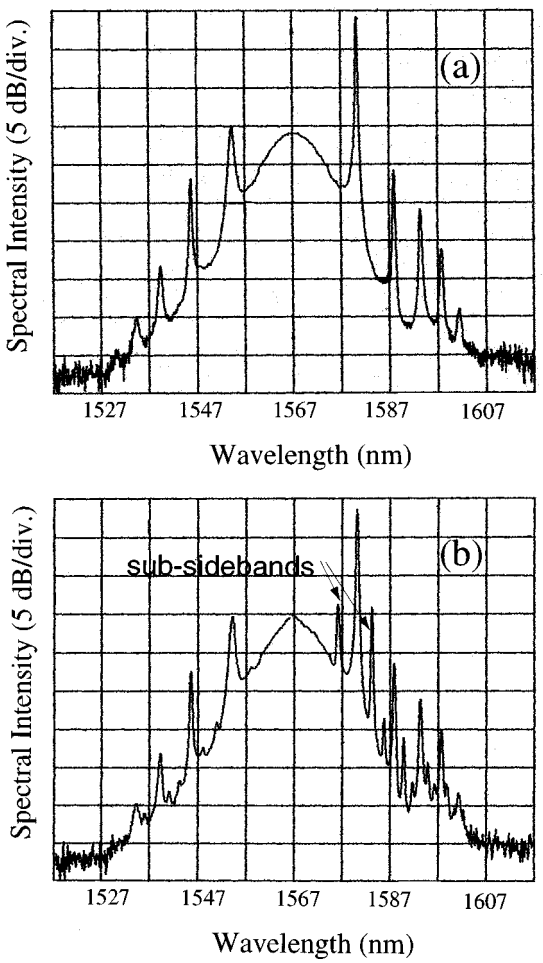

FIG. 2. Experimentally measured soliton spectra of the laser. (a) Soliton spectrum without modulational instability. (b) Soliton spectrum with modulational instability. From (a) to (b) the pump power is slightly increased. The reference levels of the spectra are the same.

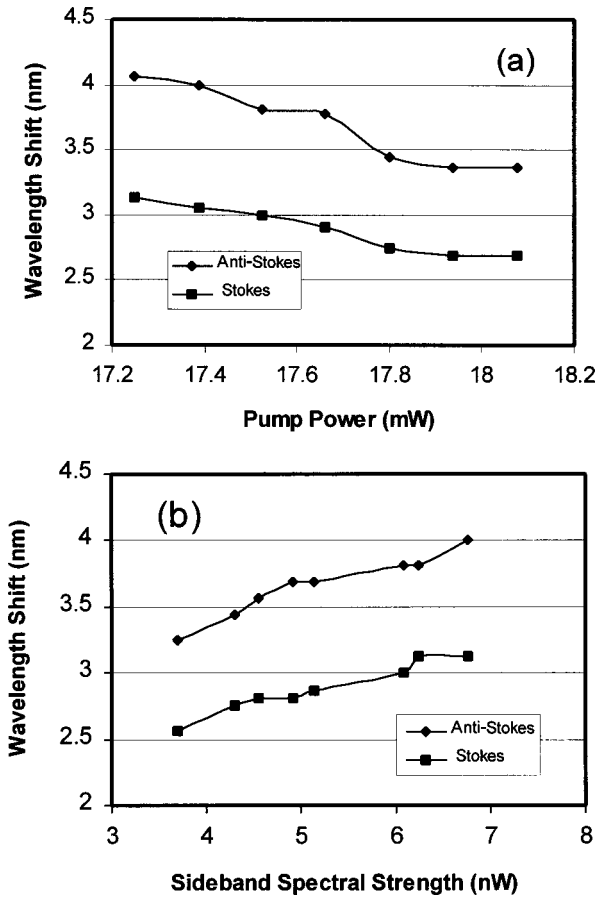

FIG. 3. Typical power tuning characteristics of the subsidebands. (a) Wavelength shift vs pump power. (b) Wavelength shift vs sideband spectral strength. Wavelength shifts are measured in relation to the corresponding unstable sideband.

lyzed with an optical spectrum analyzer and a commercial optical autocorrelator.

A common feature of fiber soliton lasers is that soliton pulses circulating in the cavity periodically experience gain and loss perturbations. Energy stability of soliton pulses is in the sense of the average energy [10]. It is a well-known fact that when the condition $Z_a \ll Z_0$ is not satisfied by the laser, where Z_a and Z_0 are the period of periodic perturbations and the soliton, respectively, sideband instability characterized by the generation of discrete spectral components in the soliton spectrum occurs in the laser [11]. Through sideband instability, soliton pulses resonantly transfer their energy, which is in excess of the energy of the average soliton, into dispersive waves. Before a new soliton pulse is created, increasing pump power will significantly increase the energy of the dispersive waves rather than the energy of the soliton pulses. Dispersive waves are linear waves. They are inherently unstable against modulational instability. When they are strong enough and beyond the modulational instability threshold, they become unstable [12].

Figure 2 shows typical soliton spectra of the laser before and after modulational instability when the central wavelength of the soliton is about 1567 nm. Figure 2(a) shows the soliton spectrum of the laser immediately before the appearance of the modulational instability. Spectral sidebands caused by the sideband instability of the laser are clearly seen in Fig. 2(a). In our experiment when the laser is in soliton operation, sideband instability is always observed. Even for the same order of sidebands, their spectral strength is significantly asymmetric, which is a result of asymmetric linear cavity loss of the laser [13]. Figure 2(b) shows the soliton spectrum after the modulational instability. From Figs. 2(a) and 2(b) the pump power is slightly increased. Comparing with the soliton spectrum shown in Fig. 2(a), Fig. 2(b) shows that new spectral components have appeared in the soliton spectrum. It can be seen in Fig. 2(b) that associated with the destabilization of a sideband, a Stokes and an anti-Stokes subsideband simultaneously appears near it. We note the large wavelength shift of the subsidebands relative to their corresponding unstable sideband. These wavelengths shifts are significantly larger than those caused by the classic modulational instability under the same sideband strength.

To show that the appearance of the new spectral subsidebands in the soliton spectrum is a result of modulational instability of the dispersive wave, we have plotted in Fig. 3

experimentally measured power-tuning characteristic of the subsidebands. The wavelength shifts of the subsidebands are measured in relation to the unstable sideband. Figure 3(a) shows the wavelength shifts versus the pump power and Fig. 3(b) versus the spectral strength of the sideband for reasons of comparison. Although the absolute wavelength shifts of the two subsidebands are different, their changes with pump power or sideband strength clearly show a similar tendency, indicating that they are two coupled components. Experimentally, with increasing pump power the spectral strength of the subsidebands always increases, whereas the strength of the unstable sideband can either decrease or increase depending on the energy transfer between it and the subsidebands. This is why in Fig. 3(a), as pump power is increased, the wavelength shifts of the subsidebands decrease. The experimental results shown in Fig. 3 suggest strongly that the wavelength shifts of the subsidebands are directly related to the sideband strength rather than the pump strength.

The modulational instability is sustained only in a very narrow range of pump power. When pump power is continuously increased, a new soliton pulse eventually forms in the laser cavity through soliton shaping of dispersive waves [14]. After a new soliton pulse is formed, the strength of the dispersive waves suddenly becomes weak and below the modulational instability threshold. Consequently, the subsidebands disappear. However, further increasing the pump power, as the strength of the dispersive waves builds up and becomes strong enough again, the modulational instability comes back, and the whole process repeats.

Although modulational instability is a threshold effect, as shown in Fig. 2 its appearance in the laser requires that the strength of a dispersive wave reaches a certain level. However, we found that once one dispersive wave in the laser has reached the instability threshold, modulational instability can also occur in the other resonant dispersive waves that have lower strength. Comparing the spectral strengths of the dispersive waves shown in Figs. 2(a) and 2(b), it is obvious that subsidebands have appeared on dispersive waves whose absolute strength is even below the modulational instability threshold. Adjusting the pump power, subsidebands associated with low strength sidebands also exhibit power-tuning characteristics. Obviously, the absolute wavelength shifts of these subsidebands are dependent also on the strength of the corresponding sidebands. The weaker the strength of a sideband, the smaller is the wavelength shift as shown in Fig. 2(b).

Since in the laser all the resonant sidebands are caused by the soliton pulse reshaping, they are coherently coupled. We believe that the appearance of the subsidebands on the low strength sidebands could be a result of the cross coupling between the sidebands. Modulational instability induced by the cross-phase-modulation has been theoretically predicted by Agrawal [15] and experimentally observed in birefringent fibers due to the coherent coupling of the two polarization modes [16]. To our knowledge, so far modulational instability induced by the cross-phase-modulation between different dispersive waves of a fiber soliton laser has not been reported.

III. NUMERICAL SIMULATIONS

To better understand the physical origins of the experimentally observed modulational instabilities, especially the modulational instability with sideband generation in the laser, we have conducted numerical simulations to study the soliton and dispersive wave dynamics of the laser. Our numerical simulations are based on the modified coupled nonlinear Schrödinger equations describing optical pulse propagation in weakly birefringent fibers [17,18]:

$$\frac{\partial u}{\partial z} = i\beta v - \delta\frac{\partial v}{\partial t} + \frac{i}{2}\beta''\frac{\partial^2 u}{\partial t^2} + i2\gamma\left(\tfrac{1}{3}|u|^2 u + \tfrac{2}{3}|v|^2 u\right) + \frac{g}{2}u, \tag{1a}$$

$$\frac{\partial v}{\partial z} = i\beta u - \delta\frac{\partial u}{\partial t} + \frac{i}{2}\beta''\frac{\partial^2 v}{\partial t^2} + i2\gamma\left(\tfrac{1}{3}|v|^2 v + \tfrac{2}{3}|u|^2 v\right) + \frac{g}{2}v, \tag{1b}$$

where u and v are the normalized envelopes of the optical pulses along the two circularly polarized modes of a birefringent optical fiber. $2\beta = 2\pi\Delta n/\lambda$ is the wave-number difference between the modes (π/β is the fiber's beat length). $2\delta = 2\beta\lambda/2\pi c$ is the inverse group velocity difference. β'' is the second-order dispersion and γ is the nonlinearity of the fiber. g is the saturable gain of the erbium-doped fiber. For undoped fiber $g = 0$. We approximate the frequency dependence of the gain by

$$g(\omega) = g_p\left[1 - \left(\frac{\omega - \omega_0}{\Omega_g}\right)^2\right], \tag{2}$$

where g_p is the peak gain, ω_0 is the peak gain frequency position, and Ω_g is the gain bandwidth.

In order to closely simulate the experimental situations, in particular considering that the experimental laser cavity comprises optical fibers of different dispersion properties, and also that the polarization controllers and the polarization-dependent isolator have discrete actions on the light beam circulating in the cavity, we have solved the laser equations in the following way. We start our numerical calculation with a weak noise light beam. We let the noise light beam circulate in the laser cavity. According to our experimental configuration, within one round trip the noise light beam will first propagate in three pieces of fibers with different group velocity dispersions. The propagation in fibers is described by the equations shown in Eqs. (1a) and (1b). Then it will pass through the polarization controllers and the polarization-dependent isolator. We modeled the action of polarization controllers and the isolator by their corresponding matrix transformation. After one round-trip propagation in the cavity, the final state is then used as the starting state for the next round of calculation. This process repeats until a stable state of the light pulse is obtained.

With this method of calculation we have explicitly taken into account the effect of nonlinear coupling between the two orthogonal polarization components of light in a birefringent fiber. The frequency-dependent nonlinear loss introduced by the combined effect of the polarization controllers and the isolator is also included in matrix transformations. We found

that the frequency dependence of the nonlinear loss was very important in correctly simulating the fiber soliton laser behavior. Taking this into account can give the details of the laser dynamics. Since every next round of numerical calculation starts with the result of calculation of the previous round as the initial condition, effects of periodic gain and loss perturbations on the soliton pulses are also automatically included in the simulation. We have performed our numerical simulations with experimental laser parameters. We found that almost all the experimentally observed behaviors of the laser can be well reproduced in the numerical simulations. In particular, we found that when the dispersion difference between the dispersion-shifted fiber and the erbium-doped fiber is considered, the numerical results can also well reproduce the modulational instabilities observed in the laser. However, with otherwise the same parameters but ignoring the dispersion difference of the fibers, the new spectral subsidebands will not appear. As an example, Fig. 4 shows a typical result of the numerical simulations. Figure 4(a) shows the case where no dispersion difference between the fibers is taken into account. In this case the sideband instability of the laser is still visible. However, no subsidebands of the dispersive waves are observed. Figure 4(c) shows the case where the dispersion difference between the fiber has been considered. Here, in contrast, subsidebands appear on the dispersive wave's spectrum. For comparison with the experimental result shown in Fig. 2, Fig. 4(b) shows the numerically calculated soliton spectrum with lower pump strength. With lower pump strength and hence weak gain, the soliton spectrum shows no subsidebands, while as the gain (pump) strength is increased, at a certain value modulational instability appears. An excellent agreement with the experimental observations is obtained. We note that in Fig. 4(c) the subsidebands also appear in the weak sidebands, indicating that it is a natural effect of the laser.

Based on the results of numerical simulations, it is clear that the observed subsideband generation is caused by the dispersion difference between the erbium-doped fiber and the other fibers used to form the laser cavity. To further understand the physical mechanism of the influence of the dispersion difference on the modulational instability, we recall that Smith and Doran have theoretically analyzed the occurrence of modulational instability in fibers with periodic dispersion management [3]. They have shown that periodic dispersion variations can modify the gain of a classic modulational instability. In particular, under small periodic dispersion variation it suppresses the gain of classic modulational instability and introduces extra large wavelength shifted gain. A fiber laser is in fact a dispersion-managed system. In a fiber laser, because the dispersion of the fibers used is different, light circulating in the cavity experiences periodic dispersion variations. We point out that although in the fiber soliton laser periodic power variation also exists, and (as shown by Matera *et al.* [5]) periodic power variations can also introduce subsideband generation of modulational instability type, our numerical simulation shows that the effect caused by it is too small, and cannot be observed in the present experimental conditions. Our numerical simulations also confirm the existence of modulational instability caused by cross-phase-modulation in the laser, as the numerical results show that subsidebands also appear on the weak resonant sidebands. This numerical result shows that strong cross-phase-modulation does exist between the sidebands.

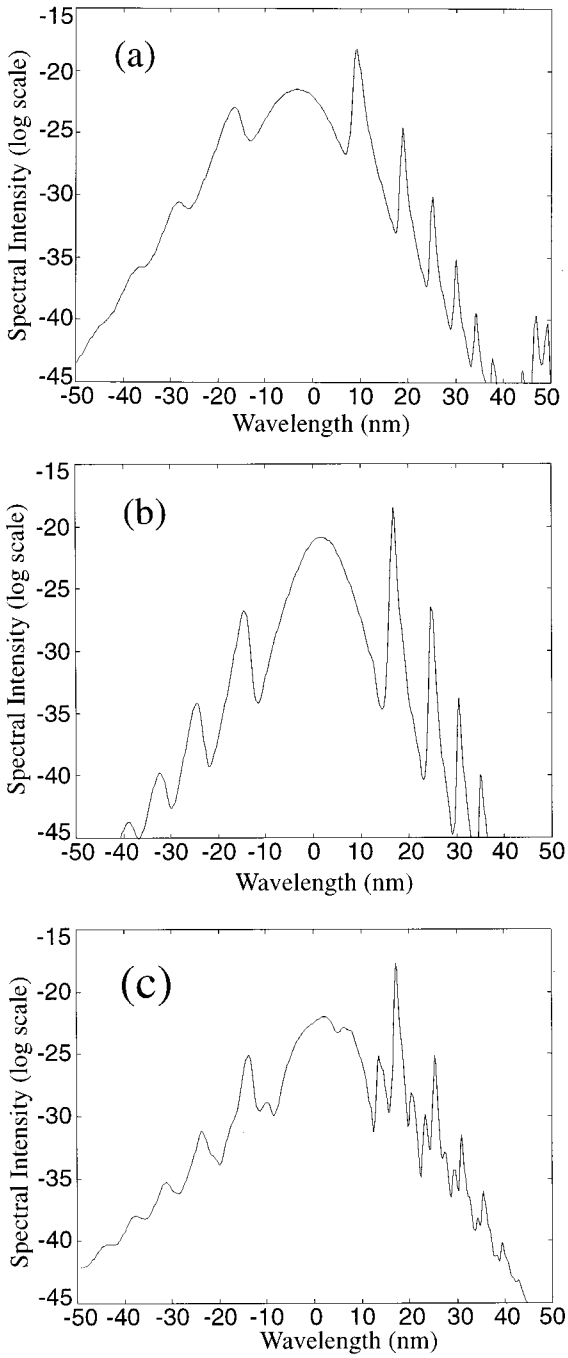

FIG. 4. Soliton spectra calculated numerically. (a) $g_p = 1400$, $\beta_1'' = \beta_2'' = -3.83$ ps/nm km. (b) $g_p = 1300$, $\beta_1'' = -2$ ps/nm km, $\beta_2'' = -10$ ps/nm km. (c) $g_p = 1400$, $\beta_1'' = -2$ ps/nm km, $\beta_2'' = -10$ ps/nm km. Other parameters used are $\Omega_g = 2\pi \times 10$ THz, $\gamma = 3\ \mathrm{W^{-1}\,km^{-1}}$, cavity length $L = 12$ m, beat length $L_b = L/5$.

IV. CONCLUSIONS

In conclusion, we have experimentally observed a modulational instability with sideband generation in a passively

mode-locked fiber soliton ring laser. We found numerically that this observed modulational instability is a result of periodic dispersion variation experienced by light circulating in the laser cavity. This periodic group velocity variation introduces extra resonances in the system, which modifies the gain spectrum of the modulational instability in fibers. Our experimental results have also revealed the existence of modulational instability caused by cross-phase-modulation in the laser. The physical mechanism of this modulational instability is the nonlinear coupling between the dispersive waves in the laser. As a result of the nonlinear phase coupling, a dispersive wave can become unstable through modulational instability, even when its strength is well below the threshold of the instability.

ACKNOWLEDGMENT

W. S. Man and H. Y. Tam acknowledge support from a university research grant from The Hong Kong Polytechnic University.

[1] K. Tai, A. Hasegawa, and A. Tomita, Phys. Rev. Lett. **56**, 135 (1986).
[2] G. Agrawal, IEEE Photonics Technol. Lett. **4**, 562 (1992).
[3] N. J. Smith and N. J. Doran, Opt. Lett. **21**, 570 (1996).
[4] K. Shiraki, T. Omae, and T. Horiguchi, *Optical Fiber Communication Conference, Vol. 2, 1998*, OSA Technical Digest Series (Optical Society of America, Washington, DC, 1998), p. 396.
[5] F. Matera, A. Mecozzi, M. Romagnoli, and M. Settembre, Opt. Lett. **18**, 1499 (1993).
[6] A. B. Grudinin, D. J. Richardson, and D. N. Payne, Electron. Lett. **28**, 67 (1992).
[7] K. Tamura, H. A. Haus, and E. P. Ippen, Electron. Lett. **28**, 2226 (1992).
[8] K. Tamura, C. R. Doerr, L. E. Nelson, H. A. Haus, and E. P. Ippen, Opt. Lett. **19**, 46 (1994).
[9] M. Hofer, M. E. Fermann, F. Haberl, M. H. Ober, and A. J. Schmidt, Opt. Lett. **16**, 502 (1991).
[10] S. M. J. Kelly, K. Smith, K. J. Blow, and N. J. Doran, Opt. Lett. **16**, 1337 (1991); A. Hasegawa and Y. Kodama, Phys. Rev. Lett. **66**, 161 (1991).
[11] S. M. J. Kelly, Electron. Lett. **28**, 806 (1992); N. J. Smith, K. J. Blow, and I. Andonovic, J. Lightwave Technol. **10**, 1329 (1992).
[12] D. Y. Tang, P. D. Drummond, W. S. Man, and H. Y. Tam, Opt. Commun. **167**, 125 (1999).
[13] W. S. Man, H. Y. Tam, M. S. Demokan, P. K. Wai, and D. Y. Tang, J. Opt. Soc. Am. A (to be published).
[14] D. Y. Tang, W. S. Man, and H. Y. Tam, Opt. Commun. **165**, 189 (1999).
[15] G. P. Agrawal, Phys. Rev. Lett. **59**, 880 (1987).
[16] S. G. Murdoch, R. Leonhardt, and J. D. Harvey, Opt. Lett. **20**, 866 (1995).
[17] C. R. Menyuk, IEEE J. Quantum Electron. **QE-23**, 174 (1987).
[18] S. G. Evangelides, Jr., L. F. Mollenauer, J. P. Gordon, and N. S. Bergans, J. Lightwave Technol. **10**, 28 (1992).